子コロイドの調製法の開発。化学工学
会第 73 年会 平成 20 年 3 月

Ⅱ. 知的財産権の出願登録状況
準備中

厚生労働科学研究費補助金（医療機器開発推進研究事業）
平成19年度　分担研究報告書

ナノサイズ・センシングカプセルの新規開発と医療応用
バイオマーカ作製

（分担）研究者　粕谷　厚生　　東北大学国際高等融合領域研究所

研究要旨
本研究では直径1nm台またはそれ以下のバイオマーカとして、CdSeナノ粒子の安定性が原子数に依存することを利用して$(CdSe)_{34}$の他に$(CdSe)_{13}$、$(CdSe)_{48}$等の原子数まで揃った安定なナノ粒子を作製する方法を開発した．特に生命体への応用を考えるにあたり，水溶性で大量合成可能な方法を見出した．

A．研究目的
発光性ナノ粒子をバイオマーカとして用いる場合は小さいほど非マーカ体の形状や動作を乱すことが避けられる．現在市販されているナノ粒子の直径は2nmを超えており，1nm台以下が求められる．しかし小さくするほど直径を揃えるのが難しくなり、特性が揃わなくなる．また発光効率も極端に落ちてしまう．表面を占める原子の数が内部に比べて極端に増えて来るために、粒子の構造を原子レベルで精密に整えることが難しくなるからである．この難問を解決するために、ナノ粒子の安定性が原子数に依存することに着目した．この性質を利用し，粒子を合成する条件に工夫を凝らすことによって特定の原子数の安定なナノ粒子が作製することが出来た．またこの試料をもいいて、発光効率も通常の粒子に比べて1000倍以上高めることも出来た．

B．研究方法
直径が1nm台になると構成原子の数は100を割り，1個の増減で安定性が大きく変化するようになる．従って粒子の成長条件によっては安定な粒子だけを選択的に合成することも可能になる．その結果成長する粒子は安定性に支配されているため、原子の数のみならず配列構造までが一意的に定まることになる．この方法により，$(CdSe)_{34}$の他に$(CdSe)_{13}$、$(CdSe)_{48}$等の原子数まで揃った安定なナノ粒子を作製することが出来た．また配列構造も揃っているため，表面修飾等によって発光効率を高められることを実際に明らかにした．

（倫理面への配慮）
該当なし

C．研究結果と考察
試料作製

先ず、Cd_2SO_4 と Na_2SeSO_3 の水溶液にCysteine 或は Thioglycerol を混ぜると1日程度で図1に示す光吸収を示す試料が成長する．Cysteine を混ぜて得た試料は波長 420nm に鋭い吸収ピークを示し，直径の揃ったナノ粒子であることがわかる．質量分析により、Octylamine で成長するのと同じ $(CdSe)_{34}$ と同定される。但し Octylamine ではピークが 415nm に観測されており，僅かながら移動しているが形状は酷似している．一方 Thioglycerol を混ぜて得た試料は 430nm に幅のある吸収ピークを示し，ある程度直径に分布のあることがわかる．

次にCdとSeの比を1:1から1:0.25に変えてCdの量を増やして同じくThioglycerolを混ぜた試料では図1に示す如くピーク波長が350nmにまで移動しており、質量分析の結果(CdSe)34 が分解して(CdSe)13の出来ることがわかった。

ナノ粒子の表面修飾と発光効率の飛躍的向上

得られた試料をクロロフォルム中で保管すると緩やかであるが日数を掛けて更に成長し、450nm付近に肩が現れると同時に415nmのピークは減少して行く。ピークの肩が長波長側に現れるのは粒子表面が修飾されて成長したためと考えられる。

この吸収の変化に対して発光を見ると当初は 420nm 付近に幅広ピークが観測されるがやがて鋭くなって強度が上がり、吸収の肩と同じ方向の長波長側に移動しながら効率は実に10,800倍にも上昇しているのがわかる。ローダミン色素と同程度の高率であることも判明した。

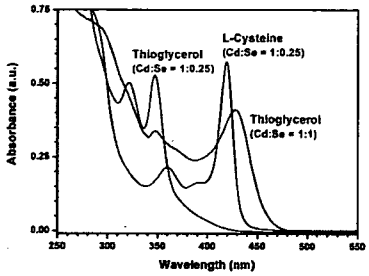

図1. 異なる条件で合成した $(CdSe)_n$ 光吸収スペクトル

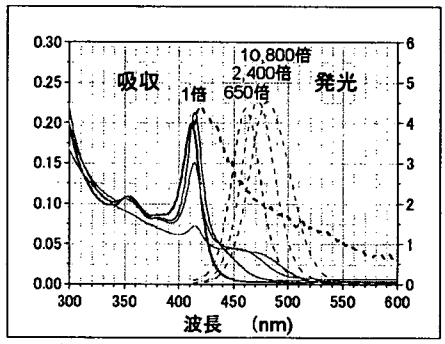

図2．クロロフォルム中に成長する $(CdSe)_n$ の発光スペクトル

F．健康危険情報

現在までのところ、本研究は人間を対象としたものではないため、健康に対する害は生じない。

G．研究発表

1. 論文発表

1) Park YS, Kasuya A, Dmytruk A, Yasuto N, Takeda M, Ohuchi N, Sato Y, Tohji, K Uo M, Watari F. Concentrated colloids of silica-encapsulated gold nanoparticles: colloidal stability, cytotoxicity, and X-ray absorption. *J. Nanosci. Nanotech.* 7

(8), 2690-2695, 2007.
2) Park YS, Dmytruk A, Dmitruk I, Noda Y, Kasuya A, Takeda M, Ohuchi N. Aqueous-phase synthesis of ultra-stable small CdSe nanoparticles. *J. Nanosci. Nanotech.* 7 (11); 3750-3753 2007
3) Zhou X, Shao Z, Kobayashi Y, Wang X, Ohuchi N, Takeda M, Kasuya A, Photoluminescence of CdSe and CdSe/CdO·nH2O Core/Shell Nanoparticles Prepared in Aqueous Solution. Optical Materials, 29, 1048-1054, 2007

H. 知的財産権の出願・登録状況

1. 特許（公開）

該当なし

2. 実用新案登録

該当なし

厚生労働科学研究費補助金（医療機器開発推進研究事業）
平成19年度　分担研究報告書

超臨界in-situ表面修飾法を用いたハイブリッドナノ粒子合成に関する研究

（分担）研究者　名嘉　節・東北大学多元物質科学研究所・准教授

要旨
本研究において、超臨界水熱合成法を用い、新規新規蛍光・X線・MRIマーカーを合成した。水中分散性を向上させるため、ガドリニウム水酸化物表面をグルコースで修飾し、粒径30nmのMRIマーカー作製に成功した。また、MRI能、蛍光およびX線CT能を有する磁性酸化物のナノ粒子化に成功した。水酸化物や新しい酸化物ナノ結晶を用いた有機-無機ハイブリッド化により高い水中分散性とナノサイズ化が可能である。

A．研究目的

高感度計測を可能とする新規蛍光・X線・MRIマーカーとして、超臨界水熱合成法を用いて、溶媒中に良分散する無機-有機ハイブリットナノ粒子を開発する。

B．研究方法

超臨界in-situ表面修飾法により、水中および溶媒中に良分散する各種蛍光・磁気ハイブリッドナノ粒子を合成する。癌組織への選択性を付与するために、ナノ粒子表面への有機分子修飾によりサイズ・形態・生体親和性を制御する。

C．研究結果

昨年度常磁性のMRIマーカーとして開発したGd水酸化のMRI能に関する基礎的な検証を行った。表面をグルコースで修飾し水中分散性を付与した場合、粒径を30nmの場合に陽性のMRIマーカーとなることがわかった。

MRI能、蛍光およびX線CT能を有する磁性酸化物のナノ粒子化に着手し、粒径数十nmの結晶合成に成功した。この粒子は希土類元素をドープすることにより蛍光マーカーとなることを確認した。これらのナノ粒子は幅広いｐH領域で重元素の溶出などが極めて少なく、有機色素とは異なり退光現象も観測されなかった。

D．考察

高い空間分解能を有するMRI能を得るためには、高い水中分散性とサイズ制御が重要である。水酸化物や新しい酸化物ナノ結晶を用いた有機-無機ハイブリッド化により高い水中分散性とナノサイズ化が可能になる。マーカーに分子様の性質を付与することにより、プロトン核磁気緩和が制御でき陽性の造影効果が得られた。

E．結論

グルコース修飾Gd水酸化物ナノマーカ

が、高空間分解能計測を可能とする陽性のMRIマーカーとなることを検証した。新しい多元マーカーとして$GdVO_4$をナノ粒子を開発した。

F．健康危険情報

現在までのところ、本研究は人間を対象としたものではないため、健康に対する害は生じない。

G．研究発表

1.　論文発表および著作

佐々木隆史，名嘉節，大原智，阿尻雅文、「蛍光特性ナノ粒子の表面修飾」（10章）『量子ドットの生命科学への応用』CMC出版 2007年.

名嘉　節，有田稔彦，阿尻雅文、「超臨界合成法による粒径制御」（第2章第2節）『ナノ粒子における電子材料・光学材料への応用』*情報技術協会*,（2007）

他２件

2.　学会発表

佐々木隆史，大原智，梅津光央，名嘉節，阿尻雅文「バイオイメージング・治療を目指した表面修飾
Gd含有ナノ粒子の超臨界水熱合成」
化学工学会第39回秋季大会，北海道，(2007.9.15)
（優秀発表賞）他2件.

H．知的財産権の出願・登録状況

なし

Ⅲ. 研究成果の刊行に関する一覧表

別紙1

雑誌論文（2007年）

発表者氏名	連名著者氏名	論文タイトル名	発表誌名	巻	号	開始頁	終了頁	出版年
Watanabe T	Sato T, Gonda K, Higuchi H	Three-dimensional nanometry of vasicle transport in living cells using dual-focus imaging optics.	Biochem Biophys Res Commun	359		1	7	2007
Mousavand T	Zhang J, Ohara S, Umetsu M, Naka T, Adschiri T	Organic-ligand-assisted supercritical hydrothermal synthesis of titanium oxide nanocrystals leading to perfectly dispersed titanium oxide nanoparticle in organic phase.	Journal of Nanoparticle Research	9		1067	1071	2007
Lima R	Wada S, Takeda M, Tsubota K, Yamaguchi T	In vitro confocal micro-PIV measurements of blood flow in a square microchannel: The effect of the haematocrit on instantaneous velocity pro files.	Journal of Biomechanics	40		2752	2757	2007
Kobayashi Y	Imai J, Ngao D, Takeda M, Ohuchi N, Kasuya A, Konno M	Preparation of multilayered silica-Gd-silica core-shell particles and their magnetic resonance images.	Colloids and Surfaces A	308	1	14	19	2007
Kobayashi Y	Misawa K, Takeda M, Ohuchi N, Kasuya A, Konno M	Control of Shell Thickness in Silica-Coating of AgI Nanoparticles.	Advanced Materials Research	29-30		191	194	2007
Park YS	Kasuya A, Dmytruk A, Yasuto N, Takeda M, Ohuchi N, Sato Y, Tohji, K Uo M, Watari F	Concentrated colloids of silica-encapsulated gold nanoparticles: colloidal stability, cytotoxicity, and X-ray absorption.	J. Nanosci. Nanotec	7	8	2690	2695	2007
Park YS	Dmytruk A, Dmitruk I, Noda Y, Kasuya A, Takeda M, Ohuchi N	Aqueous-phase synthesis of ultra-stable small CdSe nanoparticles.	J. Nanosci. Nanotec	7	11	3750	3753	2007

Zhou X	Shao Z, Kobayashi Y, Wang X, Ohuchi N, Takeda M, Kasuya A	Photoluminescence of CdSe and CdSe/CdO·nH2O Core/Shell Nanoparticles Prepared in Aqueous Solution.	Optical Materials	29		1048	1054	2007
Ishida T	Takeda M, Suzuki A, Amari M, Ohuchi N	Siginificance of irradiation in breast conserving treatment: comparison of local recurrence rates in irradiated and nonirradiated groups.	Int J Clin Oncol	13		12	17	2008
Kobayashi M	T. Mizumoto, T. Q. Duc, M. Takeda	Fluorescence Tomography of Biological Tissue Based on Ultrasound Tagging Technique	Proc. SPIE	6633		663306 -1-5		2007
Kobayashi M	K Sasaki, M Enomoto, Y. Ehara	Highly sensitive determination of transient generation of biophotons during hypersensitive response to cucumber mosaic virus in cowpea.	J. Exp. Botany Vol.	58	3	465	472	2007
Takeda M	Tada H, Higuchi H, Kobayashi Y, Kobayashi M, Sakurai Y, Ishida T, Ohuchi N	In vivo single molecular imaging and sentinel node navigation by nano-technology for molecular targeting drug delivery system and tailor made medicine.	Breast Cancer					in press
武田元博	武田元博、小林芳男、小林正樹、桜井遊、権田幸祐、樋口秀男、大内憲明	機能性ナノ粒子による生体イメージングの医療展開	ナノ学会誌					in press

別紙2

書籍（2007年度）

著者氏名	連名著者氏名	編集者名	論文タイトル名	書籍名	出版社名	出版地	出版年	開始頁	終了頁
武田元博	小林芳男、小林正樹、桜井　遊、甘利正和、石田孝宣、鈴木昭彦、大内憲明	宇理須恒雄	機能性ナノ粒子による生体イメージング―がん診療への応用―	ナノメディシン ナノテクノ医療応用	オーム社	東京	2008	64	74
樋口秀男	大内憲明	宇理須恒雄	単一量子ドットのバイオ・医療ナノイメージング	ナノメディシン ナノテクノ医療応用	オーム社	東京	2008	52	63
佐々木隆史	名嘉節、大原智、阿尻雅文		蛍光特性ナノ粒子の表面修飾	量子ドットの生命科学領域への応用	シーエムシー出版社	東京	2007	115	121

別紙3

学会発表 (2007年度)

国内

2008年春季第55回応用物理学関係連合講演会
異分野融合ナノテクノロジー横浜コロキウム、平成20年2月1日、横浜
武田元博、樋口秀男、大内憲明
機能性ナノ粒子の医学領域における展開

第17回乳癌基礎研究会、平成19年7月28-29日、大阪
武田元博、桜井遊、小林芳男、叢莉蔓、甘利正和、亀井尚、石田孝宣、鈴木昭彦、菅原旭浩、大内憲明
ナノサイズヨウ化銀ビーズの腫瘍とセンチネルリンパ節のX線CT造影効果

第66回日本癌学会学術総会、2007年10月、横浜
Motohiro Takeda, Hideo Higuchi & Noriaki Ohuchi
Nano-imaging of single quantum dots and nano-particles in mice tumor.

第66回日本癌学会学術総会、2007年10月、横浜
Kawai M, Higuchi H, Takeda M and Noriaki O
In Vivo Imaging of Vascular Permeability Using Nanocrystals in Mice Tumor.

ナノ学会第5回大会、2007年5月、つくば市
河合賢朗, 樋口秀男, 大内憲明
マウス腫瘍新生血管における透過性のIn vivo imaging.

第107回日本外科学会総会、2007年4月、大阪
甘利 正和、石田 孝宣、武田 元博、鈴木 昭彦、宇佐見 伸、多田 寛、大内 憲明
進行・再発乳癌におけるカペシタビンの治療効果の検討

第15回日本乳癌学会学術総会、2007年6月、横浜
甘利正和、石田孝宣、武田元博、鈴木昭彦、大内憲明
若年者乳癌の臨床病理学的検討

第15回日本乳癌学会総会、2007年6月、横浜
大内憲明, 多田寛, 河合賢朗, 武田元博, 石田孝宣, 樋口秀男
生体超微細1分子可視化によるナノDDSと乳癌標的治療

平成19年東北地区若手研究者研究発表会, 講演番号YS-5-50, 講演資料p. 79 (2007)
大原健, 鈴木祐輔, 水本喬, 榎本幹, 武田元博, 小林正樹
超音波タグ蛍光イメージング法による生体試料の蛍光断層計測

平成19年東北地区若手研究者研究発表会, 講演番号YS-5-08, 講演資料p. 15 (2007)
山内崇弘, 渡邉尚哉, 小林正樹

超高感度CCDを用いたヒト生物フォトンイメージングによる皮膚酸化ストレス計測の検討

平成19年東北地区若手研究者研究発表会, 講演番号YS-5-09, 講演資料p. 17 (2007)
菊地大輔, 千葉朋子, 小林正樹
極微弱発光による化学反応波の動態計測とイメージング

平成19年東北地区若手研究者研究発表会, 講演番号YS-5-10, 講演資料p. 19 (2007)
熊坂増高, 内堀綾斗, 武田元博, 亀井尚, 桜井遊, 大内憲明, 小林正樹
がん転移診断のためのセンチネルリンパ節蛍光イメージング法の検討ーブタを用いた腹腔内視鏡による観

国際(海外)

SASAKI T, OHARA S, UMETSU M, NAKA T, ADSCHIRI T
Supercritical Hydrothermal Synthesis of Hybrid Gd(OH)3 Nanoparticles : Application to Neutron
The 1st international symposium on supercritical fluid synthsis and materials, Beijing, China, Mar.2007

Kawai M, Higuchi H, Ohuchi N.
Trastuzumab regulates receptor recycling on cancer cell.
The 9th International Symposium of Future Medical Engineering based on Bio-manotechnology, Sendai, January 7-9, 2007.

Cong L, Takeda M, Ohuchi N.
Silica coated nano-particles for biomedical contrast imaging.
The 9th International Symposium of Future Medical Engineering based on Bio-manotechnology, Sendai, January 7-9, 2007.

Li-Shishido S, Watanabe T, Tada H, Kawai M, Higuchi H, Ohuchi N. Reduction in nonfluorescence state of quantum dots on an immunofluorescence staining.
The 9th International Symposium of Future Medical Engineering based on Bio-manotechnology, Sendai, January 7-9, 2007.

Tada H, Higuchi H, Watanabe T, Ohuchi N.
In vivo imaging using quantum dots in mice.
The 9th International Symposium of Future Medical Engineering based on Bio-manotechnology, Sendai, January 7-9, 2007.

Sakurai Y, Takeda M, Kasuya A, Kobayashi Y, Kamei t, Amari M, Cong L, Ohuchi N.
Nano size silver iodide beads as novel contrast media for sentinel lymph node navigation surgery.
The 9th International Symposium of Future Medical Engineering based on Bio-manotechnology, Sendai, January 7-9, 2007.

Takeda M, Tada H, Kawai M, Sakurai Y, Higuchi H, Ohuchi N,
In vivo Single Molecular Imaging and Sentinel Node Navigation using Nano-biotechnology for Medical

The 3rd Tohoku-NUS Symposium on Nano-Biomedical Engineering in the East Asian-Pacific Rim Region, 10-11 Dec 2007, National University of Singapore

Kawai M, Takeda M, Higuchi H, Ohuchi N,
Tumor Interstitial Nano-particle Delivery and Analysis in the Human Tumor Xenograft in Mice.
The 3rd Tohoku-NUS Symposium on Nano-Biomedical Engineering in the East Asian-Pacific Rim Region, 10-11 Dec 2007, National University of Singapore

Hamanaka Y, Takeda M, Tada H, Kawai M, Sakurai Y, Amari M, Suzuki A, Ishida T, Ohuchi N,
In vivo tracking of anti-cancer drugs and the active sites conjugated with quantum dots.
The 3rd Tohoku-NUS Symposium on Nano-Biomedical Engineering in the East Asian-Pacific Rim Region, 10-11 Dec 2007, National University of Singapore

Sakurai Y, Takeda M, Cong L, Amari M, Kasuya A, Kobayashi Y, Kamei T, Ohuchi N,
In vivo Distribution of Silver Iodide Beads in Cancerous Legions.
The 3rd Tohoku-NUS Symposium on Nano-Biomedical Engineering in the East Asian-Pacific Rim Region, 10-11 Dec 2007, National University of Singapore

Duc TQ, Mizumoto T, Nanbu Y, Takeda M, Kobayashi M,
Tomographic Imaging of Fluorophore Embedded in Biological Tissue Based on Ultrasound Tagging
The 7th pacific Rim Conference on Lasers and Electro-Optics (CLEO), Abstract pp.1193-1194 (Seoul, Korea)(August, 2007)

Kawai, M., Higuchi, H., Gonda, K., Takeda, M., and Ohuchi, N.
In vivo imaging of vascular permeability using nano-objects in mice tumor.
2nd "Hot Topics in Molecular Imaging - TOPIM" meeting of the European Society for Molecular Imaging. February 2008 Grenoble, France.

Ohuchi, N., Takeda, M., Kawai, M., Tada, H. Sakurai, Y., Gonda, K., and Higuchi, H.
Novel imaging techniques with functional nano-objects for cancer diagnosis.
2nd "Hot Topics in Molecular Imaging - TOPIM" meeting of the European Society for Molecular Imaging. February 2008 Grenoble, France.

Ⅳ. 研究成果の刊行物・別刷

Available online at www.sciencedirect.com

ScienceDirect

Biochemical and Biophysical Research Communications 359 (2007) 1–7

BBRC

www.elsevier.com/locate/ybbrc

Three-dimensional nanometry of vesicle transport in living cells using dual-focus imaging optics

Tomonobu M. Watanabe [a,1], Takashi Sato [b], Kohsuke Gonda [a], Hideo Higuchi [a,*]

[a] *Biomedical and Engineering Research Organization, Tohoku University, Sendai, Miyagi 980-8579, Japan*
[b] *Department of Materials Science, Graduate School of Engineering, Tohoku University, Sendai, Miyagi 980-8579, Japan*

Received 11 April 2007
Available online 4 May 2007

Abstract

Dual-focus imaging optics for three-dimensional tracking of individual quantum dots has been developed to study the molecular mechanisms of motor proteins in cells. The new system has a high spatial and temporal precision, 2 nm in the x–y sample plane and 5 nm along the z-axis at a frame time of 2 ms. Three-dimensional positions of the vesicles labeled with quantum dots were detected in living cells. Vesicles were transported on the microtubules using 8-nm steps towards the nucleus. The steps had fluctuation of ~20 nm which were perpendicular to the axis of the microtubule but with the constant distance from the microtubule. The most of perpendicular movement was not synchronized with the 8-nm steps, indicating that dynein moved on microtubules without changing the protofilaments. When the vesicles changed their direction of movement toward the cell membrane, they moved perpendicular with the constant distance from the microtubule. The present method is powerful tool to investigate three dimensional movement of molecules in cells with nanometer and millisecond accuracy.

Keywords: Nanotechnology; Step size; Dynein; 3D; Kinesin

Motor proteins such as dynein, kinesin, and myosin play roles in cell motility such as vesicle transport, mitosis, and muscle contraction [1,2]. To describe the mechanisms of motility at a molecular level, single molecule studies including *in vitro* motility assay have been used [3–7]. Despite all the *in vitro* measurements performed using purified motor proteins in artificial solutions, it is important to investigate the motility of these proteins in living cells because physiological conditions in the cell environment are very different to those in *in vitro* assays [8–10].

In living cells, cytoplasmic dynein transports vesicles bound to its tail domain via membrane associated proteins [1]. The single particle imaging and tracking techniques using fluorescence dyes such as GFP or quantum dots observed the behavior of the vesicles in cells with nanometer and millisecond accuracies [7,9]. Dynein and kinesin transport vesicles with successive 8 nm steps in living cells [11–13] which is the same as that *in vitro* [7,14]. Many questions, however, have arisen about the *in vivo* behaviors of the motor proteins. Is dynein responsible for switching the protofilaments? Is the vesicle transport obstructed by the cytoskeletal network [1,2]? Since the motor proteins are arranged and work three-dimensionally (3D) in cells, it was difficult to answer these questions from results obtained by measurements of the movements viewed in two dimensions under a conventional microscope.

In the previous works, 3D tracking of particle movements has been constructed by moving the focal position by changing the position of an objective [15–17]. However, the method is not suitable for tracking fast biological pro-

* Corresponding author. Fax: +81 22 217 5753.
E-mail address: higuchi@tubero.tohoku.ac.jp (H. Higuchi).
[1] Present address: PREST, Japan Science and Technology Agency, Kawaguchi, Saitama, Japan.

0006-291X/$ - see front matter © 2007 Elsevier Inc. All rights reserved.
doi:10.1016/j.bbrc.2007.04.168

cesses that occur in a millisecond time scale because of the limitations of the speed of moving the objective. To overcome this problem, we developed a new optical method of dual view optics, which allows us to visualize three-dimensional biological processes with high temporal (2 ms) and spatial (2–5 nm) precisions without moving the objective. Using this technique we observed the inward transport of the membrane protein labeled with quantum dots (QDs) presumably by dynein in living cells.

Materials and methods

DIO (dual-focus imaging optics) system. The optical system for DIO consisted of an epi-fluorescent microscope (IX-71, Olympus), an EM camera (Ixon DV860, Andor), and a Piezo actuator having a electrostatic sensor (FB010-C, Nanocontrol). An area $\sim 10 \times 10\ \mu m^2$ was illuminated by a green laser (532 nm, 0.1 $mW/\mu m^2$ for each specimen, Big Sky laser) using diagonal irradiation [13]. The fluorescence of the quantum dots was filtered using a high-pass filter (transmission wavelength >580 nm; Omega). The Piezo actuator moved the position of the objective by the Piezo driver having a positional feedback loop (NC1100, Nanocontrol). We analyzed the data in which root-mean-square noise was <10 nm.

Preparation of anti-HER2-QDs and cells. HER2 (human epidermal growth factor receptor 2) on the membrane was labeled with multiple quantum dots via an anti-HER2 antibody according to the method reported previously [13]. Human breast cancer cells, KPL-4 cells, were cultured on a coverslip in DMEM (Gibco) containing 5% FBS (fetal bovine serum, Gibco) at 37 °C in 5% CO_2. Just prior to the experiment, FBS was removed for an hour to starve the cells, and the quantum dot-anti-HER2 antibodies were added to the cells [13]. To observe steps clearly, the experiments of 3D imaging were performed at low temperature 16–18 °C under the epi-fluorescence microscope with DIO system [13].

Results and discussion

DIO (dual-focus imaging optics) system and 3D single particle tracking

In order to track the 3D movement of single fluorescent particles, we developed a new optical system that two separated images at distinct focal positions were taken with an EM-CCD camera, called DIO (Fig. 1A). A narrow image of a sample on an epi-fluorescence microscope went through a slit positioned at the imaging surface ("Slit" in Fig. 1A). The optical pathway was split into two pathways by a half mirror (HM in Fig. 1A). Moving either L3 or L4 along the optical axis produced a difference between the two pathlengths. The difference in the optical lengths resulted in the difference in the focuses and magnification of the two images on the camera (an inset image in Fig. 1A). The distance between the two focal positions was set to ~1 μm in the present study and the ratio of magnification of the two pathways was ~0.96 (Supplement 1). The two images of a quantum dot were fitted to 2D Gaussian functions [13]. The difference in the fluorescence intensities at the centroid of the functions fit to was plotted as the function of z-position of the quantum dots (Fig. 1C). This curve was taken before every experiment as a calibration curve (Fig. 1C). The x–y position of a quantum dot was determined by fitting the images with 2D Gaussian functions as previously reported [6,7,9,13]. The spatial resolution was highly dependent on the number of photons emitted from a fluorophore [18]. Quantum dots were used in this study because of their superior fluorescence durabil-

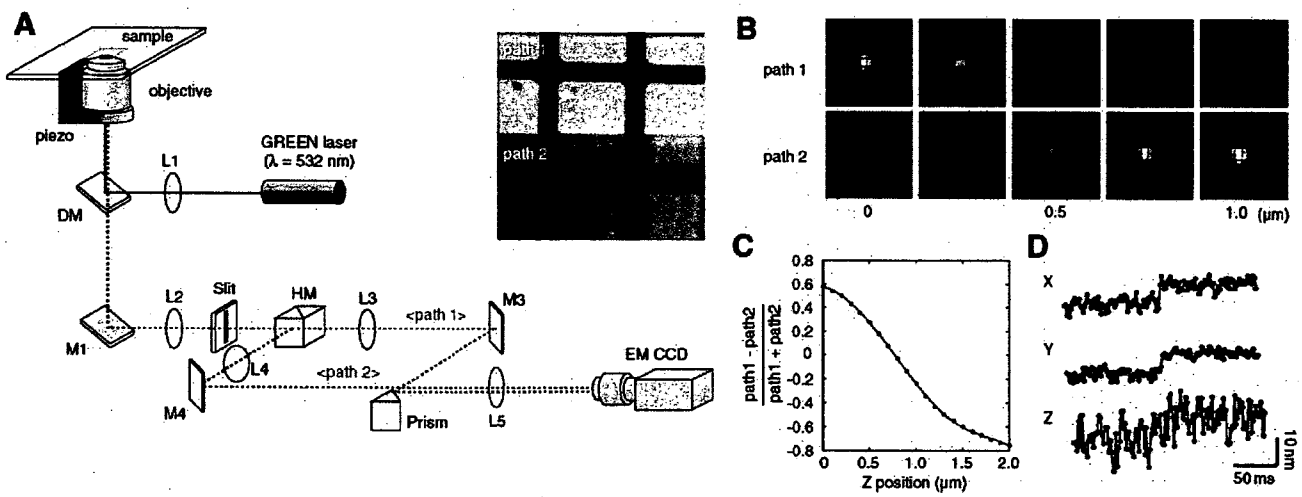

Fig. 1. Three-dimensional single particle tracking. (A) Schematic drawing of an optical set up for dual-focus imaging (DIO). A Piezo actuator bound to the objective. L, lens; M, mirror; DM, dichroic mirror; HM, half mirror cube. An inset panel shows an image of a test pattern of a square lattice (10 μm). Upper image is an image just in focus. (B) Fluorescent images at two distinct focus positions (path 1 and path 2). Quantum dot is located between the two focusing positions. An objective was moved along the optical axis (z-axis). (C) Calibration curve of z-position vs difference of the fluorescent intensities. The fluorescent intensities were recorded as the quantum dots moved along the z-axis. The division of the difference between the intensities in the two pathways and the addition of them was represented as (path 1 − path 2)/(path 1 + path 2). When quantum dots were moved in cells, z-position in the calibration curve was multiplied by the refractive index ratio, 0.88, of water, 1.33 to oil, 1.52. (D) Accuracy of the present methods. Quantum dot(s) fixed on a coverslip were moved by 10 nm steps using a Piezo actuator. The position of the Quantum dot(s) was determined with a temporal resolution of 2 ms with noise of 2.0 nm (x-axis and y-axis) and 5.3 nm (z-axis).

ity [7,13,19,20]. The spatial precisions of the dots fixed on a coverslip using the 3D tracking system were 2.2, 1.5, and 5.3 nm on the x, y, and z directions, respectively, with time resolution of 2 ms (Fig. 1D).

3D vesicle transport in living cells

In order to observe 3D movements of vesicles in living cells, quantum dots coated with anti-HER2 antibodies (human epidermal growth factor receptor 2) were mixed with breast cancer cells, KLP-4, which overexpresses HER2 on the cell membrane. Microtubule-based transport of the vesicles labeled with quantum dots (QD-vesicles) in the cytosol were visualized using diagonal illumination (Fig. 2A) [13]. The QD-vesicles moved in one direction i.e. towards the nucleus (Fig. 2B and Movie S1), and occasionally moved away from the nucleus to the cell membrane. The fluorescence intensity in dual images changed with time (Fig. 2B); for example, intensities on the left panels in Fig. 2B were low at 0 and 3 s and high at 1.2 s. These indicate the movement of z direction. QD-vesicles moved on GFP-microtubules as observed by confocal microscopy (Movie S2), confirming that the vesicles were indeed transported by a microtubule-based motor, either dynein or kinesin. Movements of QD-vesicles presumably by dynein from the cell membrane to the peri-nuclear region were also recorded. The moving QD-vesicles transported in 3D space were successfully monitored for a precision of a few nanometers on xy-plane and several nm on z-axis with 2 ms resolution using the DIO system (Fig. 2C and D).

How does dynein walk on a microtubule three-dimensionally with nanometer accuracy while transporting a vesicle? Smooth traces of the displacements were produced by averaging 100 points over a 200 ms period to follow the overall pathways of the QD-vesicles roughly. All of the smooth traces ($n = 57$) were then fitted approximately to the planes. Thirty-eight traces (67%) could be well fitted to a single plane with the standard deviation of the distance between the traces and the fitted plane being <10 nm (mean = 4.6 nm) (Fig. 3A). If artificial random traces were fitted to a plane (Supplement 2A), the standard deviation of the distance was not less than 10 nm ($n = 100$, Supplement 2B). Thus, the planar movements were not part of the random movements. Twelve traces (21%) could not be fitted by a single plane, but were well fitted to two or

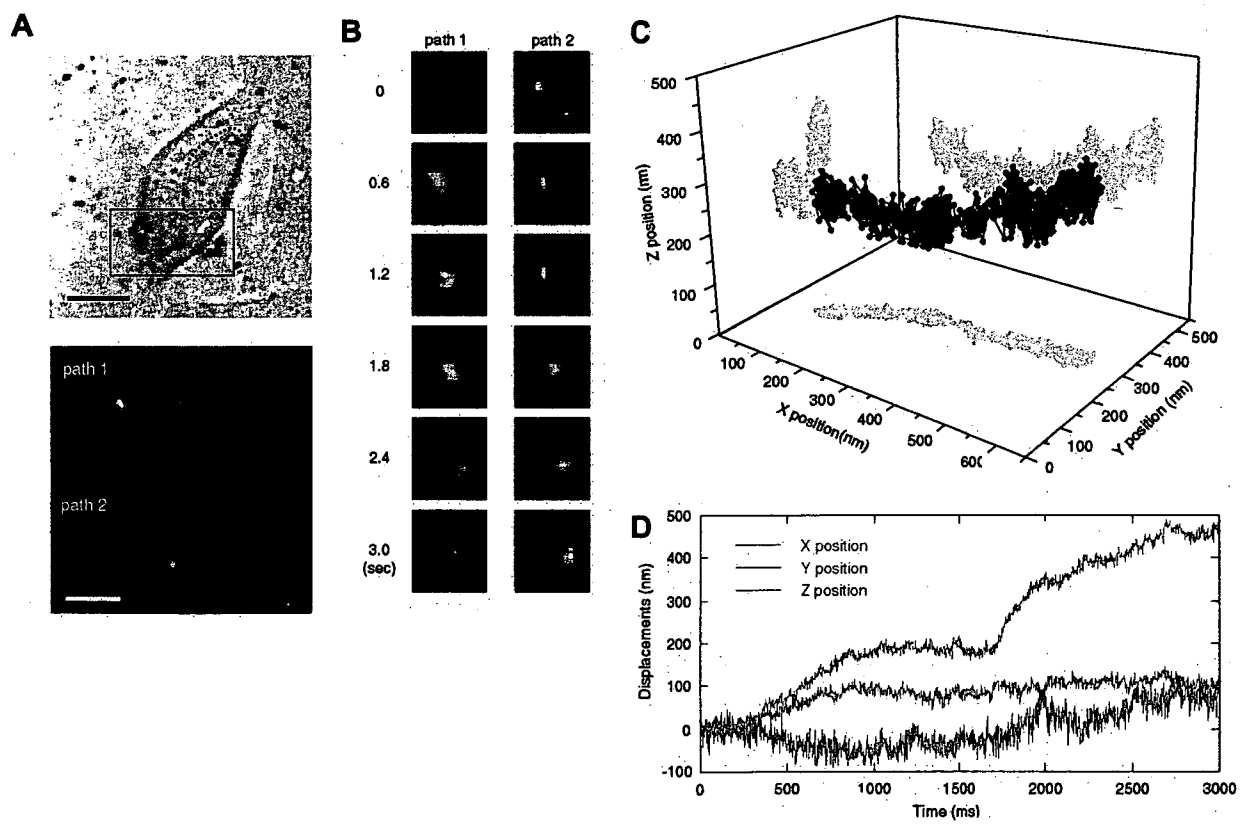

Fig. 2. Three-dimensional tracking of a moving vesicle in a living cell. (A) A bright field image (upper) and fluorescence images (lower) obtained using DIO. The red rectangle indicates the fluorescent imaging area. The fluorescent images of vesicles labeled with quantum dots were in the cell at two distinct focus positions. Yellow arrowheads indicate the vesicle being transported towards the nucleus. Calibration bars were 10 μm in a upper panel and 5 μm in a lower one. (B) Time course of the fluorescent images of the moving vesicle indicated by the yellow arrowheads in (A). The vesicle moved to the right, which is the direction towards the peri-nuclear region. (C) 3D movements of the transport of the QD-vesicle towards the peri-nuclear region. Six colors from blue to green indicate the running time from 0 to 3 s (0.5 s each color). (D) The time courses of x (red), y (blue), and z-positions (green) in (C).

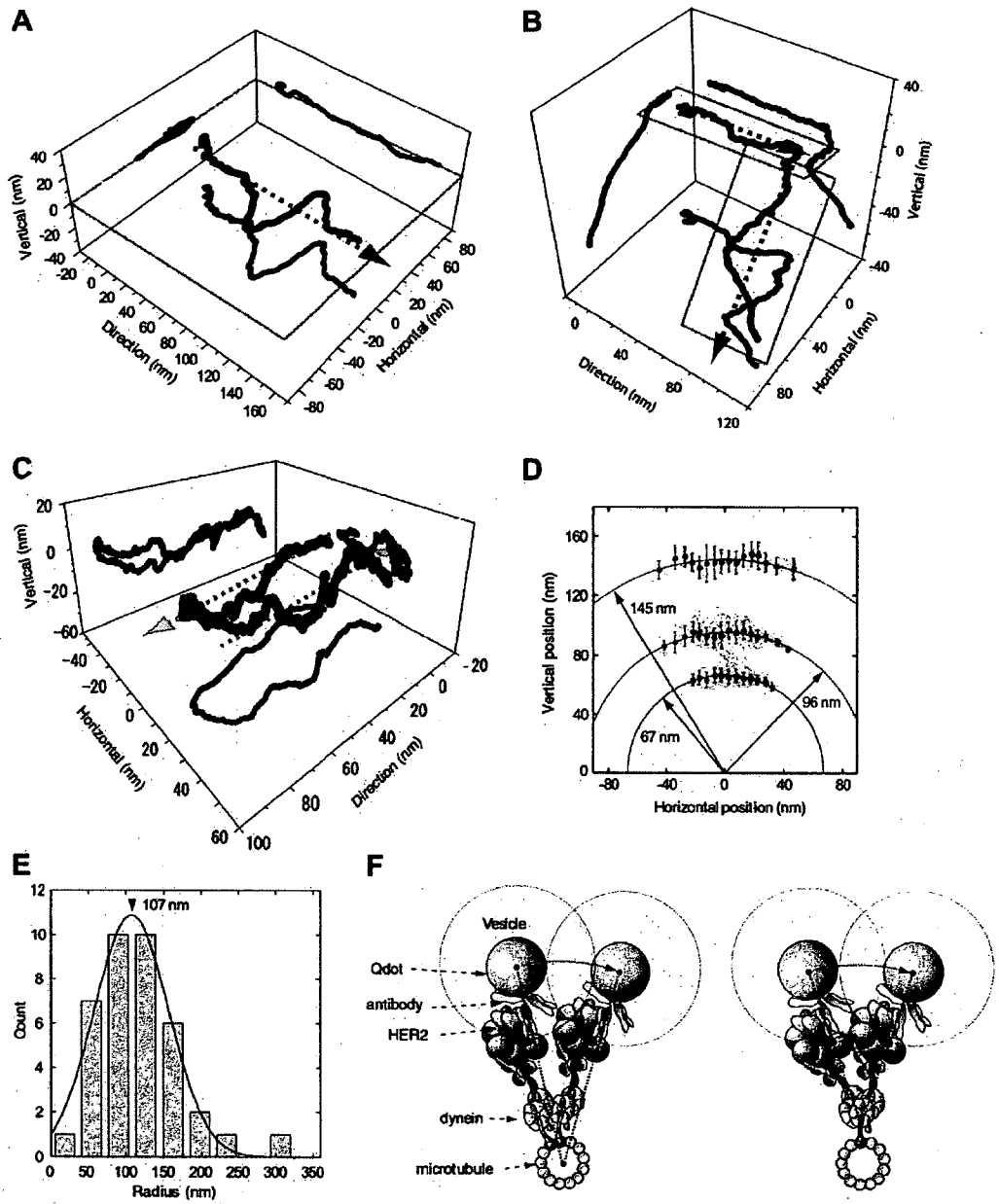

Fig. 3. Movement of the vesicle transport by dynein in living cells. (A) Typical traces of the movements in the different planes. The traces were well fitted with a primary plane surface ($f(x,y,z) = ax + by + cz + d$; a, b, c, and d are the fitting parameters (cyan line). (B) Typical trace when QD-vesicle transfers from one microtubule to another microtubule. The trace was fitted well to two planes. Cyan lines indicate the data have been fitted by two planes. (C) A typical trace of the directional switching by most likely dynein and kinesin. (D) Vertical–horizontal plots of the 3D traces. The graph shows the typical three traces (red, blue, and green). Plots and bars indicate the average values taken every 5 nm along the horizontal axis and the standard deviations, respectively. Traces were fitted with a circle. Cyan arrows in (A), (B), and (C) indicate the direction of movement of the vesicles. (E) Histogram of the radius of the cylindrical surfaces. The distribution followed to a Gaussian distribution with a peak of 107 ± 49 nm (red line, $n = 38$). (F) Possible models to explain the cylindrical movements of the vesicle during transportation. The left panel shows the model where dynein transfers from one protofilament to another on a microtubule. The right panel shows the model that dynein did not transfer but fluctuate around the binding site of dynein and tubulin.

three planes with standard deviations <10 nm (Fig. 3B). The remaining seven traces could not be distinguished from random movement because of the large standard deviations (>10 nm). Helical type movements were not observed in any of the traces.

An abrupt change in the direction of movement of the vesicles was observed in three traces (5%) which are fitted to one plane. In all cases, the QD-vesicles moved by 30–50 nm in the horizontal direction in a stepwise fashion when the direction of movement suddenly changed to the opposite direction (Fig. 3C and Fig. 3S). Kinesin is a motor that moves vesicles to the plus-end of a microtubule and is thought to be involved in this process by directly competing with dynein [12].

Three-dimensional nanometry of vesicle transport

To examine the systematic displacement of quantum dots from the planes, the vertical position displaced from the plane and horizontal positions perpendicular to moving direction were repotted (Fig. 3D). These plots could be well fitted to arcs, a part of a circle. The mean radius of the arcs was determined to be 107 nm (Fig. 3E). The arcs indicate the distance between the center of a microtubule and the center of quantum dots because the distance, 107 nm, is consistence with the distance estimated from the radius of a microtubule (13 nm), the length of the dynein (50–80 nm), the length of the membrane protein and antibody complex (10–20 nm) and the radius of a quantum dot (~12 nm) (Fig. 3F) [21,22]. The approximately planar or exactly arc movements suggest that vesicles were transported on single microtubules. The traces which fitted to two or three planes suggest that vesicles can switch from one microtubule to another during vesicle transport.

Movement in the horizontal axis (~20 nm in S.D.) was much larger than movement in the vertical axis (~4 nm) (Fig. 3D). There are two possibilities that could explain the large movements in the horizontal plane. One is that dynein steps onto the neighboring protofilaments (Fig. 3F, left) [22]. This is suggested from studies that recombinant yeast dynein was shown to step to neighboring protofilaments in the *in vitro* assays [14]. In this model, the horizontal movement should occur at steps in travel direction. The other possibility is that the flexible linker, stalk or tail, in dynein allows the quantum dot to fluctuate around the linker (Fig. 3F, right) [23–25]. In this model, the horizontal movement does not need to occur at the directional steps.

To distinguish between these two possibilities, the step sizes of the QD-vesicles in directional, horizontal, and vertical movements were analyzed (Fig. 4). Steps were detected in the directional and the horizontal orientation using our computing algorithm (Fig. 4A, red and blue lines) [13], while steps in the vertical orientation was within a few nanometers which is not distinguished from the noise. The histogram of the step sizes in the directional orientation showed three distinct Gaussian distributions with the main peak occurring at 8.1 nm and minor peaks at 16 and −8 nm (Fig. 4B). The histogram of the pairwise distances also confirmed that 8 nm steps occurred in the directional movement (Fig. 4C) [3]. The 8 nm unitary steps were

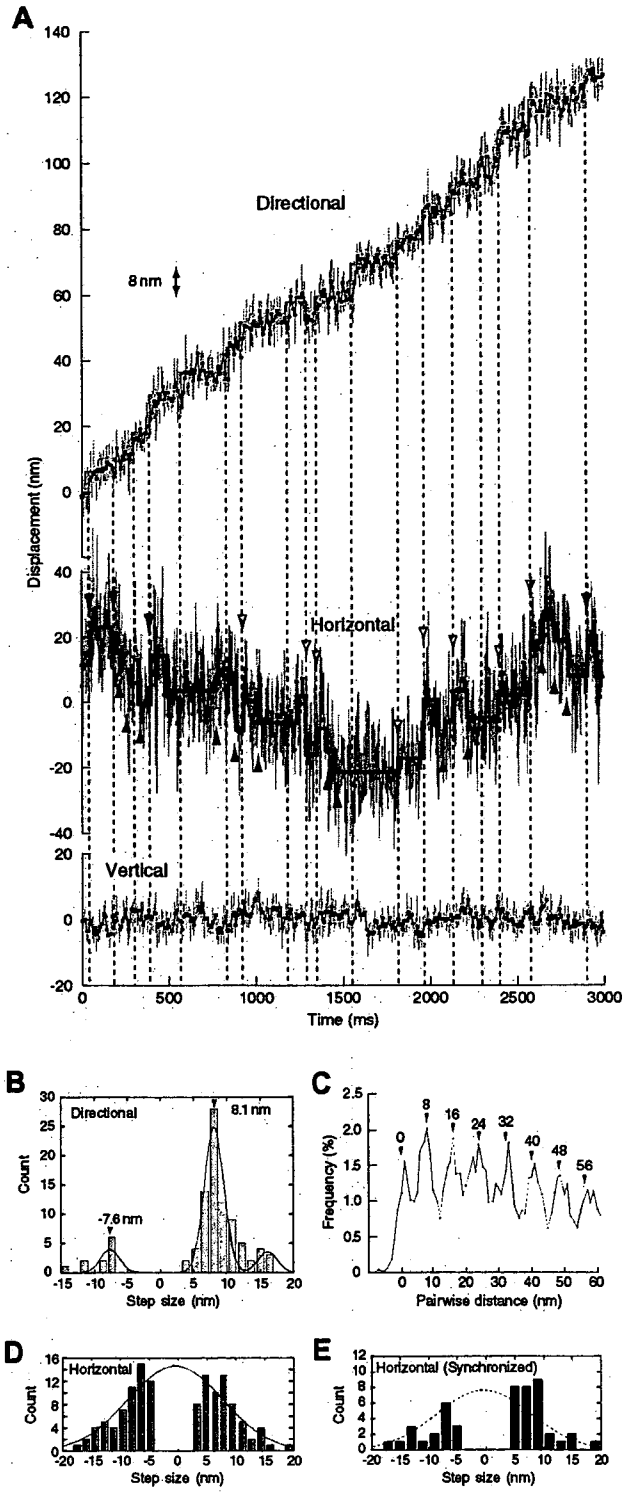

Fig. 4. Three-dimensional nanometry of a moving vesicle. (A) The typical time courses in the directional, horizontal, and vertical axes. Data points of the displacements were analyzed at 2 ms intervals (Gray lines). Five points were then averaged to smoothen the traces as shown by black squares and lines. A step size larger than 4 nm was detected here by the computer algorithm [13]. Broken lines indicate the moments where the 8 nm steps occured along the directional axis. Yellow arrowheads indicate the steps are not in synchronization with the directional 8 nm steps. (B) Histogram of the step size in the directional axis. The graph was fitted with multiple Gaussian functions. The peaks ± widths are 8.1 ± 1.5 nm at forward steps and −7.6 ± 1.4 nm at backward steps. (C) Histogram of the all pair wise distance analysis [3] (40 ms interval) of the trace in directional axis shown in (A). (D) Histogram of the step size in the horizontal axis. The graph was fitted with a Gaussian function with the peak of 0.5 nm and a width of 8.2 nm. (E) Histogram of the step size in the horizontal axis when horizontal steps were in synchronization with the directional 8 nm steps. Dotted line indicates the Gaussian curve the same as that in (D).

consistent with the value previously determined in two dimensions in living cells [7,11–14].

Some of horizontal steps synchronized with the directional 8 nm steps (Fig. 4A, blue arrowheads), but many of them did not (yellow arrowheads). The sizes of both synchronized and non-synchronized steps were fitted to a Gaussian distribution with the peak at 0.5 nm and a standard deviation of 8.2 nm (Fig. 4D and E). The horizontal step sizes of 8.2 nm were much smaller than ~50 nm which was estimated from the model that describes dynein changing the protofilaments during movement. These results suggest that dynein primarily moves on certain protofilaments in the microtubules with small fluctuation around the microtubule. In a living cell, there are many obstacles such as other vesicles, organelles, and the cytoskeletal meshwork that will prevent vesicle transport from moving in a straight line along a protofilament on a microtubule. Dynein may be able to subtly change the structure of the flexible linker to encounter obstacles (Fig. 3F, right).

The horizontal step size of 30–50 nm in Fig. 3C (Supplement 3) was comparable to the horizontal step size of ~50 nm predicted from Fig. 3F (left), suggesting that these two motors, presumably dynein and kinesin, move on distinct protofilaments or bound to a vesicle separatedly.

Here, we successfully observed vesicle transport in three dimensions in living cells with nanometer and millisecond accuracy using the DIO system. We found that dynein primarily walks in straight lines on a protofilament of a microtubule and changes protofilaments minor. The lateral displacement of QD-vesicles can be explained by the flexible linker region in the dynein molecule, and this would contribute to the robustness of the dynein-based vesicle transport through the cytoskeletal meshwork filled with organelles and other vesicles without having to switch to other protofilaments. The present method is powerful tool to investigate many kinds of 3D movement of molecules in cells with nanometer and millisecond accuracy.

Acknowledgments

We gratefully acknowledge J.M. West for critical reading this manuscript. This work was supported by Grants-in-Aid for Scientific research in Priority Areas from the Japan MEXT (H.H.), Special Coordination Funds for Promoting Science and Technology of JST (H.H., K.G. and T.M.W.) and CREST of JST (H.H.).

Appendix A. Supplementary data

Supplementary data associated with this article can be found, in the online version, at doi:10.1016/j.bbrc.2007.04.168.

References

[1] N. Hirokawa, Kinesin and dynein superfamily proteins and the mechanism of organelle transport, Science 279 (1998) 519–526.
[2] R.-I. Tuxworth, M.A. Titus, Unconventional myosins: anchors in the membrane traffic relay, Traffic 1 (2000) 11–18.
[3] K. Svoboda, C.-F. Schmidt, B.-J. Schnapp, S.-M. Block, Direct observation of kinesin stepping by optical trapping interferometry, Nature 365 (1993) 721–727.
[4] T. Funatsu, Y. Harada, M. Tokunaga, K. Saito, T. Yanagida, Imaging of single fluorescent molecules and individual ATP turnovers by single myosin molecules in aqueous solution, Nature 374 (1995) 555–559.
[5] A. Ishijima, H. Kojima, T. Funatsu, M. Tokunaga, H. Higuchi, H. Tanaka, T. Yanagida, Simultaneous observation of individual ATPase and mechanical events by a single myosin molecule during interaction with actin, Cell 92 (1998) 161–171.
[6] A. Yildiz, J.-N. Forkey, S.-A. McKinney, T. Ha, Y.-E. Goldman, P.-R. Selvin, Myosin V walks hand-over-hand: single fluorophore imaging with 1.5-nm localization, Science 300 (2003) 2061–2065.
[7] S. Toba, T.-M. Watanabe, L. Yamaguchi-Okimoto, Y.-Y. Toyoshima, H. Higuchi, Overlapping hand-over-hand mechanism of single molecular motility of cytoplasmic dynein, Proc. Natl. Acad. Sci. USA 103 (2006) 5741–5745.
[8] Y. Sako, J. Ichinose, M. Morimatsu, K. Ohta, T. Uyemura, Optical bioimaging: from living tissue to a single molecule: single-molecule visualization of cell signaling processes of epidermal growth factor receptor, J. Pharmacol. Sci. 93 (2003) 253–258.
[9] A. Yildiz, P.-R. Selvin, Fluorescence imaging with one nanometer accuracy: application to molecular motors, Acc. Chem. Res. 38 (2005) 574–582.
[10] Y. Chen, B.-C. Lagerholm, B. Yang, K. Jacobson, Methods to measure the lateral diffusion of membrane lipids and proteins, Methods 39 (2006) 147–153.
[11] C. Kural, H. Kim, S. Syed, G. Goshima, V.-I. Gelfand, P.-R. Selvin, Kinesin and dynein move a peroxisome in vivo: a tug-of-war or coordinated movement? Science 308 (2005) 1469–1472.
[12] X. Nan, P.-A. Sims, P. Chen, X.-S. Xie, Observation of individual microtubule motor steps in living cells with endocytosed quantum dots, J. Phys. Chem. B, Condens Matter Mater. Surf. Interfaces Biophys. 109 (2005) 24220–24224.
[13] M.-T. Watanabe, H. Higuchi, Stepwise movements in vesicle transport of HER2 by motor proteins in living cells, Biophys. J., 92 (2007) 4109–4120.
[14] S.L. Reck-Peterson, A. Yildiz, A.P. Carter, A. Gennerich, N. Zhang, R.D. Vale, Single-molecule analysis of dynein processivity and stepping behavior, Cell 28 (2006) 335–348.
[15] I.-M. Peters, Y. van Kooyk, S.-J. van Vliet, B.-G. de Grooth, C.-G. Figdor, J. Greve, 3D single-particle tracking and optical trap measurements on adhesion proteins, Cytometry 36 (1999) 189–194.
[16] V. Levi, Q. Ruan, E. Gratton, Melanosomes transported by myosin-V in Xenopus melanophores perform slow 35 nm steps, Biophys. J. 88 (2005) 2919–2928.
[17] T. Ragan, H. Huang, P. So, E. Gratton, 3D particle tracking on a two-photon microscope, J. Fluoresc. 16 (2006) 325–336.
[18] R.-E. Thompson, D.-R. Larson, W.-W. Webb, Precise nanometer localization analysis for individual fluorescent probes, Biophys. J. 82 (2002) 2775–2783.
[19] A.-P. Alivisatos, Semiconductor clusters, nanocrystals, and quantum dots, Science 271 (1996) 933–937.
[20] X. Michalet, F.-F. Pinaud, L.-A. Bentolila, J.-M. Tsay, S. Doose, J.-J. Li, G. Sundaresan, A.-M. Wu, S.-S. Gambhir, S. Weiss, Quantum dots for live cells, in vivo imaging, and diagnostics, Science 307 (2005) 538–544.
[21] O.-I. Wagner, J. Ascano, M. Tokito, J.-F. Leterrier, P.-A. Janmey, E.-L. Holzbaur, The interaction of neurofilaments with the microtubule motor cytoplasmic dynein, Mol. Biol. Cell 15 (2004) 5092–5100.